

Correlation and Keying of Rayleigh Scatter for Loss and Temperature Sensing in Parallel Optical Networks

Mark Froggatt, Brian Soller, Dawn Gifford and Matthew Wolfe

Luna Technologies, 2020 Krafi Drive, Blacksburg, VA 24060
froggattm@lunatechnologies.com

Abstract:

We develop a method by which coherent optical frequency domain reflectometry (OFDR) can be used to “key” portions of optical fiber by measuring their complex Rayleigh backscatter signatures. We show that these complex keys can be used to locate specific fiber lengths embedded within a parallel optical network, and that they can further be used to interrogate any induced loss or temperature change in the identified portion of the network.

1. Introduction

Optical Time-Domain Reflectometry (OTDR) is a widely used tool for identifying problems in large optical networks by providing long-range, low-resolution measurements of the level of scatter versus distance along the link. Optical Frequency Domain Reflectometry (OFDR) provides similar data, but at higher resolution over shorter ranges (tens of microns of resolution over tens of meters of range).¹⁻³ This change in distance scale allows OFDR to be used in module- and submodule-level diagnostics. As we show here, the ability of OFDR to measure the complex spectral reflectivity of Rayleigh backscatter as a function of length yields surprising new and potentially quite useful results.

When couplers are used in a network, reflectometric interrogation from one side of a coupler produces a measurement in which the backscatter from the two output legs of the coupler is combined into a single trace (see Fig. 1). Although scattering events and losses can be identified, one cannot determine from simple OTDR or OFDR measurements in which fiber specific events occurred. Without the ability to distinguish different branches of a network, it is possible to identify a faulty component in a network and, in the attempt to cut it out of the network for replacement, inadvertently cut another unrelated fiber, thus prolonging the repair. In many cases, then, knowledge of which fiber caused a loss event would be very helpful in achieving a quick and efficient repair of the system.

In what follows, we show that the full complex data available from OFDR measurements of Rayleigh backscatter make it possible to 1) localize a loss *and/or* a temperature change event on the far side of a coupler within one of the two possible output fibers, and 2) positively identify a particular segment of fiber in a larger, *parallel* optical network. Using prior complex OFDR measurements of fiber segments, hereafter referred to as reference “keys,” one can identify the location and characteristics of these segments in a larger network, even in the presence of overlapping signals. This concept is illustrated in Fig. 1, where red and blue reference keys are used to determine that a tight bend occurs in the leg of the coupler containing the red fiber segment.

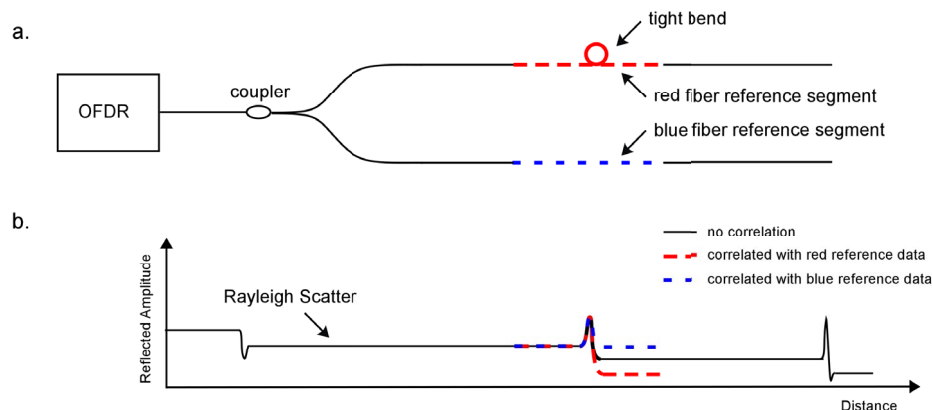


Fig. 1 (a). Diagram of a simple 2x2 coupler network. (b). Representation of an OFDR measurement of the scatter from the network in part (a). The solid black line represents the nominal measurement in which scatter from both legs of the coupler is combined in a single trace. The dashed red and blue lines represent the scatter data when correlated with reference data from the red and blue legs of the coupler respectively.

2. Analysis

Let's imagine we are going to "key" two fibers that are color coded red and blue by their Rayleigh scattering signatures. The Rayleigh backscatter signatures of both fibers as a function of distance are $\sigma_{red0}(z) = \rho_{red0}(z)e^{i\phi_{red0}(z)}$ and $\sigma_{blue0}(z) = \rho_{blue0}(z)e^{i\phi_{blue0}(z)}$. When the two scattering fields are superimposed (as they will be when connected to the two split leads of a coupler), the amplitude of the scattering will be,

$$\begin{aligned} |\sigma_{sum}(z)|^2 &= |\sigma_{red0}(z - z_{red})|^2 + |\sigma_{blue0}(z - z_{blue})|^2 + \\ &\sigma_{red0}(z - z_{red})\sigma_{blue0}^*(z - z_{blue}) + \sigma_{blue0}(z - z_{blue})\sigma_{red0}^*(z - z_{red}). \end{aligned} \quad (1)$$

From Eq. 1, one can see that there is a component of the total scatter amplitude of the system that is highly correlated to both original red- and blue-fiber scatter patterns. When a cross-correlation is performed between $|\sigma_{red}(z)|^2$ and $|\sigma_{sum}(z)|^2$, a large peak will occur at $z = z_{red}$, locating the red fiber segment. The two original scattering patterns thus act as reference keys that can be used to locate a particular fiber segment, even in the presence of other scattering elements.

If we physically alter the red fiber—through bending loss, for example—this will impose a slowly varying envelope upon the scatter from that segment of fiber. If we assemble the network in Fig. 1. and measure the scatter through the coupler it will have the form,

$$\sigma_{coupler}(z) = \Delta_{red}(z)\rho_{red0}(z)e^{i\phi_{red0}(z)+i\delta_{red}(z)} + \rho_{blue0}(z)e^{i\phi_{blue0}(z)}. \quad (2)$$

where the relative change in amplitude and phase between the original data sets and the newly measured data set is given by Δ and δ respectively. If we then multiply the data set taken through the coupler by the complex conjugate of red fiber key, shifted by the appropriate amount to align with the fiber segment in the new data set (as determined by the cross-correlation mentioned above), we get

$$\sigma_{coupler}(z)\sigma_{red0}^*(z) = \rho_{red0}^2(z)\Delta_{red}(z)e^{i\delta_{red}(z)} + \rho_{red0}(z)\rho_{blue0}(z)e^{i\phi_{blue0}(z)-i\phi_{red0}(z)}. \quad (3)$$

Note that the term associated with the red segment of fiber now contains only the slowly varying phase term, δ_{red} . If we examine the phasors associated with the red and blue terms over a region where δ_{red} remains approximately constant, we see that the red phasors line up along a single phase angle while the blue term (the second term in Eq. 3) produces phase vectors at random angles. For lengths where Δ and δ are approximately constant, we see that the expected value of the blue term's amplitude is zero while the expected value of the amplitude of the red term is the average value of the red amplitude, as shown in Eq. 4. The expected value of the red phase is the presumed static phase change, δ_{red} .

$$\left\langle \left[\sigma_{redx}(z) + \sigma_{bluex}(z) \right] \sigma_{red0}^*(z) \right\rangle = \left\langle \rho_{red0}^2(z) \right\rangle \left\langle \Delta_{red}(z) \right\rangle \left\langle e^{i\delta_{red}(z)} \right\rangle = \left\langle \rho_{red0}^2 \right\rangle \Delta_{red} e^{i\langle \delta_{red} \rangle} \quad (4)$$

From this we can see that averaging the data produced using Eq. 3 over a large number of points isolates the amplitude and phase effects that are associated with the red fiber.

For data obtained in this fashion, loss events will be reflected in the amplitude data. However, if a fiber is heated or cooled, the scattering amplitude will be largely unaffected. Instead, the phase term will accumulate a linearly growing difference due to the thermo-optic effect. The rate of change of the phase data can therefore be used as an indicator of temperature change, as shown in Fig. 4.

3. Demonstration

In order to demonstrate these capabilities, we color coded two fibers, red and blue, and then measured their Rayleigh scatter patterns over a 20 nm wavelength range centered at 1555 nm using the OFDR network described in Ref. 4. From each fiber, we selected a 0.66 m region of scatter to act as a reference key. We then spliced the two sections of fiber to the two outputs of a 1x2 fused coupler.

Following this, we induced a sharp bend in the middle of the red fiber (see Figure 1) and measured the combined network. The amplitude data for this measurement is shown in Figure 2. We then located the two previously measured segments by cross-correlation with the stored red and blue keys. The data measured through the coupler was then multiplied by the appropriately shifted reference keys in turn. The complex data sets produced by each multiplication were then low-pass filtered. The amplitudes of these data sets are shown in Figure 3. While the increase in backscatter at the sharp bend bleeds through to the blue data, the data on the other side of the bend shows that there is loss in the red fiber rather than the blue.

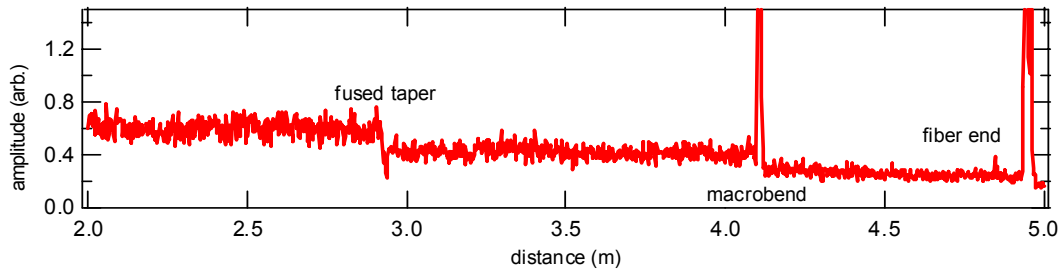


Fig. 2 Reflection amplitude as a function of length from the coupler network shown in Fig. 1

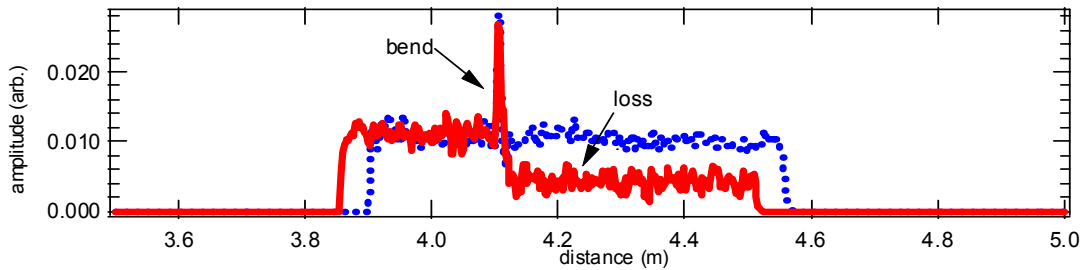


Fig. 3 Reflection amplitude correlated with the red (solid) and blue (dotted) fiber “keys” in the vicinity of the macrobend. Note that even though the signals overlap, the loss can be not only located, but associated with the red fiber.

In order to demonstrate temperature discrimination, we chose to cool a section of the blue fiber using a commonly available cold item found in our refrigerator. After placing the item in contact with the blue fiber, a new data set was taken and processed as described above. Figure 4 shows both the amplitude and phase derivative of the blue and red data sets. As expected, the amplitudes of both measurements are largely unaffected while the phase derivative of the blue fiber is dramatically altered.

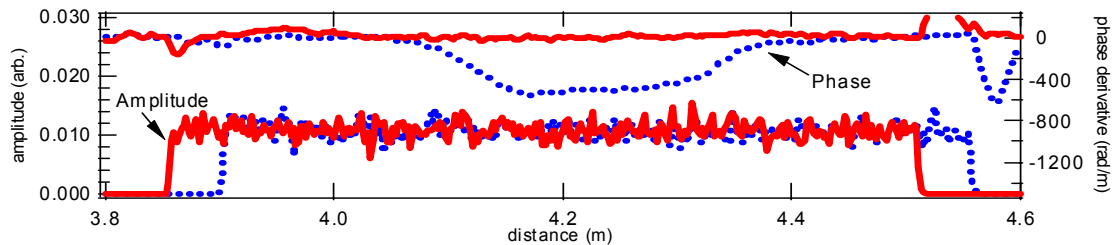


Fig. 4 Reflection amplitude and phase derivative data correlated with the red fiber section (solid) and the blue fiber section (dotted) with a cooling element applied to the blue fiber section. The change in local phase derivative locates cooled section of fiber..

4. Conclusion

In conclusion, we have demonstrated a measurement technique that provides accurate complex Rayleigh scatter measurements. We have also shown that these measurements can be used to identify specific sections of fiber within a network as well as the loss between the observation point and the fiber section. Further, localized loss events or changes in fiber temperature are also readily identified. At a time when fiber-optic assembly and testing remains a challenge, this capability, when combined with automation could provide a one-connect method for verifying network assembly and quality.

5. References

1. U. Glombitza and E. Brinkmeyer, *J. Lightwave Technol.*, **11**, 1377-1384, 1993
2. J. P. von der Weid *et al.*, *J. Lightwave Technol.*, **15**, 1131-1141, 1997
3. M. Froggatt and J. Moore, *Applied Optics*, **37**, 1735-1740, 1998.
4. B. J. Soller and M. E. Froggatt, BGPP 2003, paper MB4, *OSA Special Meeting on Bragg Gratings, Photosensitivity and Poling in Glass Waveguides*, Sept. 2003.